Transactions of JWRI, Vol. 37 (2008), No. 1

High Rate Zinc Oxide Film Deposition by Atmospheric TPCVD Using Ar/Air Plasma Jets†

ANDO Yasutaka*, KOBAYASHI Akira, TOBE Shogo* and TAHARA Hirokazu*****

Abstract

In order to develop a functional film deposition process with a high deposition rate, as a basic study, deposition of zinc oxide film by atmospheric thermal plasma CVD (TPCVD) was carried out. As feedstock, working gas and substrate, ethanol diluted zinc acetate solution, Ar and 430 stainless steel were used. As for the deposition conditions, Ar gas flow rate was fixed at 20SLM, deposition distance (distance between substrate surface and nozzle outlet of plasma torch) was fixed at 100 and 150 mm. Consequently, 100 μm thick photo-catalytic zinc oxide film could be obtained by only 5 min. deposition. Besides, by addition of air to Ar plasma jet, high enthalpy plasma jets could be obtained. From these results, this technique is found to have high potential for high rate and low cost zinc oxide film deposition.

KEY WORDS: (Thermal Spray) (Surface Modification) (CVD, Photo-catalyst) (Zinc Oxide)

1. Introduction

Zinc oxide has been widely used for antibacterial coating, LED[1], FED (Field emission display)[2], dye-sensitized solar cell[3] and transparent electrode[4] as well as conventional UV cut coating, arrester, piezo-electric device because of its excellent photo-electric property and electrical conductivity with transparency. Especially, when the zinc oxide is used as FED, film shaped zinc oxide is desired rather than powder shaped one.

As the film deposition method, sputtering[5], CVD[6] and a sol-gel process[7] have been practically used. How-ever, sputtering and CVD have some disadvantages such as the necessity of vacuum equipment, low deposition rate, and the sol-gel process also has some problems, for example difficulty of thick film deposition due to break down by internal stress occurring during deposition and so on. Although thermal spraying has been widely used as a high rate thick film deposition process in the atmospheric environment, difficulty of film component and structure control and high ingredient powder cost need to be solved in this process. Therefore, development of a high rate film deposition method using simple equipment is desired.

In this study, in order to develop high rate film deposition process which can control structure and components of the film and obtain photo-catalytic film with high strength, as a basic study, deposition of zinc oxide film was conducted.

2. Experimental Procedure

The TPCVD apparatus consisted of plasma torch, DC power supplying system, micro tube pump (starting material supplying system) and working gas supplying system as shown in **Fig.1**. The plasma torch has water cooled electrodes. The anode is made from copper, has an alkoxide feeding port at the head and has the constrictor which is 6 mm in diameter. A cylindrical cathode made from 2 % thoriated tungsten has a diameter of 3 mm. Ar was used as the working gas. Mass flow rate of the gas was fixed at 20 SLM. As the starting material for zinc oxide film deposition, ethanol diluted zinc acetate ($(CH_3COO)_2Zn$) water solution (25% zinc acetate water solution) was used. Substrates were 15mm x 15mm x 1mmt 430 stainless steel plates with grit blasted surfaces. The substrate was horizontally set on the substrate holder and the central area of the sample was placed as the axial center of the plasma jets irradiating this sample. The distance between the nozzle outlet of the plasma torch and the surface of the substrate was varied from 100 mm to 150 mm. The deposition time was 5 min. The discharge power was 25 V, 175 A. After zinc oxide film deposition, investigations of the microstructures of

† Received on July 11, 2008
* Ashikaga Institute of Technology
** Associate Professor
*** Osaka Institute of Technoplogy

Transactions of JWRI is published by Joining and Welding Research Institute of Osaka University, Ibaraki, Osaka 567-0047, Japan.

the films by X-ray diffraction (CuKa, 40 kV, 100 mA), pencil scratch test of the film deposited substrate in order to confirm the adhesion strength. Besides, in order to confirm photo-catalytic property of the film, hydrophilic test and methylene-blue decoloration test, shown in **Fig.2**, were carried out. The deposition conditions are shown in **Table 1**.

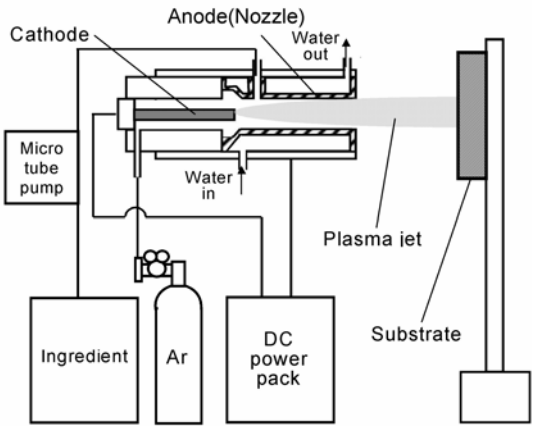

Fig.1 Schematic diagram of TPCVD apparatus.

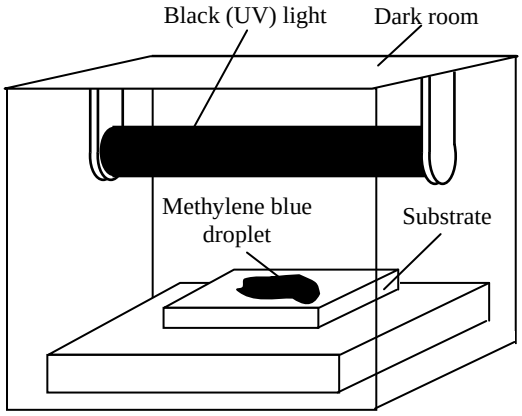

Fig.2 Illustration of the Methylene-blue decoloration test.

Table 1 Experimental conditions.

Working gas	Ar
Working gas flow rate	20 l /min
Discharge Current	175A
Discharge Voltage	25V
Deposition distance	100～150mm
Deposition time	6 min
Feedstock	C_2H_5OH diluted $(CH_3COO)_2Zn$) solution
Ingredient feed rate	200 ml /h
Substrate	430 stainless steel

3. Results and Discussion

3.1 Zinc oxide film deposition by atmospheric thermal plasma CVD

Fig.3 shows appearances of the plasma jets at the normal state and starting material injection state. Although the length of the plasma jets was 20 mm and a light green flame due to copper ion was observed at the head of the plasma jets in case of Ar plasma jet (without zinc acetate injection), the length was elongated to over 100 mm and the color was turned into orange due to some ions derived from the feedstock in case of the starting material injection state. **Fig.4** shows optical micrograph of the fracture cross-section of the zinc oxide film deposited at the condition of 100 mm in deposition distance. As shown in this figure, over 70 μm thick columnar structure film could be formed by only 5 min. deposition.

3.2 Effect of deposition distance on zinc oxide film

Since a thermal plasma has steep axial and radial profiles, deposition distance is one of the most important operation conditions affecting the film structure and its components. **Figs.5, 6** show the appearances, XRD patterns of the samples for the conditions of 100 mm,

Fig.3 Appearance of feedstock material injected Ar plasma jet in the case of non-cooled nozzle use.

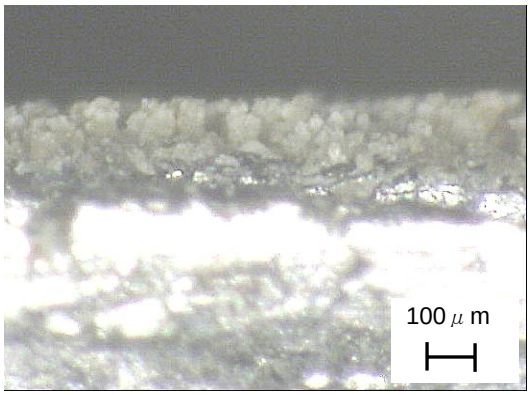

Fig.4 Optical micrograph of fracture cross-section of the zinc oxide film deposited sample.

150 mm in deposition distance. Deposition temperatures on the conditions 100 mm, 150 mm in deposition distance were approximately 773 K and 723 K, respectively. As for the appearance of the sample, each one shows almost the same appearance. However, degree of crystallinity of the film deteriorated as the deposition distance became long. Although steep ZnO peaks are detected in the cases of 100 mm and 150 mm in deposition distance, ZnO peaks became broad in the case of 200 mm in deposition distance. As for the variation of degree of crystallinity, the reason should be confirmed from the view point of nucleation of the feedstock during flight in the plasma jet as well as deposition temperature.

As photo-catalytic property detection method, wettability test and methylene-blue decoloration test are relatively easy methods. In this section, the results from these tests are reported. **Fig.7** shows appearances of the samples before and after methylene-blue decoloration test. The films were hydrophilic in the cases of the films deposited at the condition of 100 mm in deposition distance, though the film indicated water slightly repellent in the case of 150 mm in deposition distance. Besides, all of them could decolor methylene-blue after 8 hour UV irradiation. In particular, the film at the condition of 100 mm could decolor perfectly.

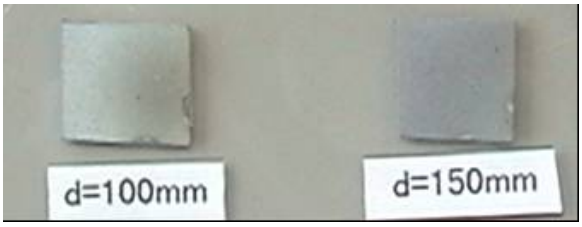

Fig.5 Appearances of the zinc oxide film deposited samples. (d: Deposition distance)

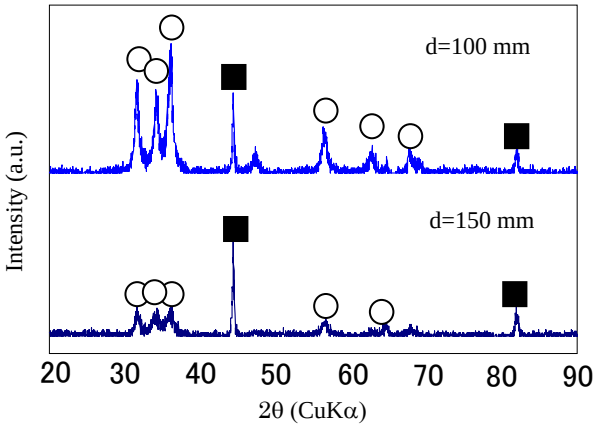

Fig.6 XRD patterns of the zinc oxide films.
d: Deposition distance
○: ZnO, ■: Fe (Substrate)

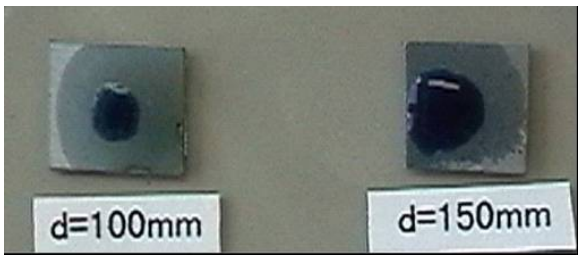

a) Before UV irradiation

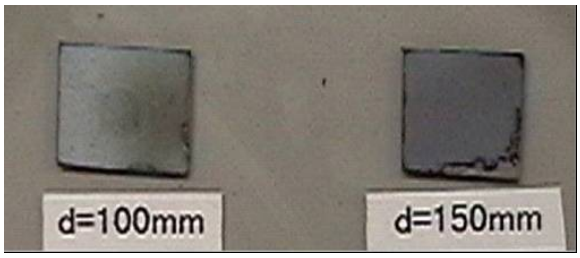

b) After 8 hour UV irradiation

Fig.7 Results of methylene-blue decoloration test. (d: Deposition distance)

3.3 Effect of air addition as carrier gas

Fig.8 shows the appearance of the feedstock injected plasma jet on each condition of air addition. The plasma jet turned from purple into yellow, and the length of the jet became short with increasing air mass flow. Since the interval time of feedstock supply became short with increasing air mass flow and the feedstock supply was continuous on the condition of 10 SLM in additional air mass flow (Q_{air}=10 SLM), air addition to the plasma jet was thought to be useful for continuous feedstock supply. However, the vaporized feedstock became liquidized during flight because the plasma jet was cooled by air addition at the condition of Q_{air}>10 SLM. **Figs.9, 10** show appearances and fracture cross-sections of the zinc oxide film deposited substrates at the conditions of Q_{air}=0 (Ar plasma jet) and 10 SLM. As shown in these figures, the microstructure of the film seems to be varied from granular to columnar by the additional air though no difference could be confirmed as for the appearances. The microstructure variation is thought to occur due to the variation of axial flow field and continuity of feedstock supply. **Fig.11** shows XRD patterns of these films. Since both films were ZnO dominant films, it was proved that the influence of the degree of the plasma jet cooling by the additional air could be negligible at the condition of Q_{air}=10 SLM though the effect of air addition on Zinc oxide film component could not be confirmed at these conditions. Besides, though deterioration of degree of crystallinity of the Zinc oxide film occurs in the case of Q_{air}=0 SLM, all deposited films had the same quality in the case of Q_{air}=10 SLM.

Q_{air}=10 SLM

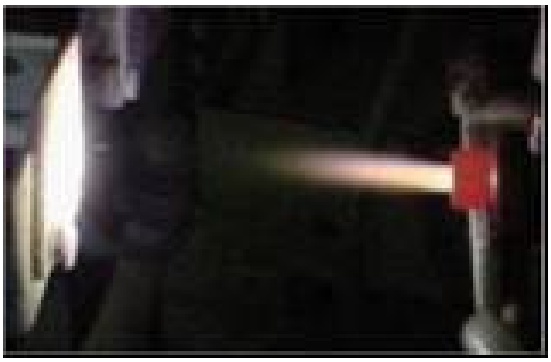

Q_{air}=20 SLM

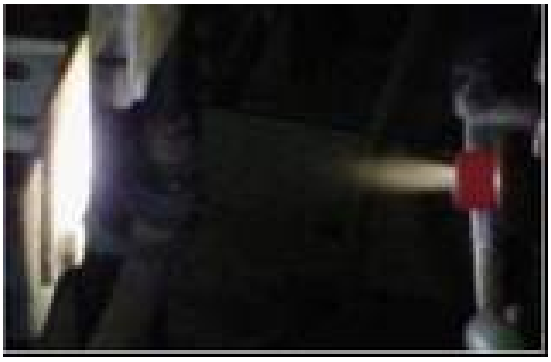

Q_{air}=40 SLM

Fig.8 Appearance of feedstock material injected Ar plasma jet on the condition of each air flow rate.

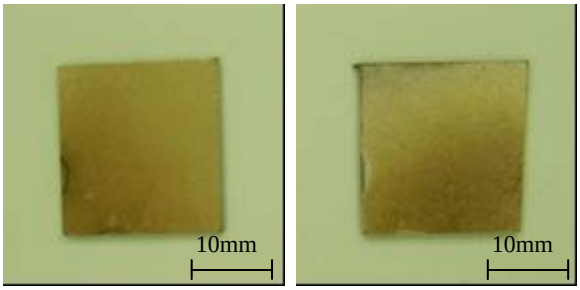

Q_{air}=0 SLM Q_{air}=10 SLM

Fig.9 Appearances of the zinc oxide film deposited substrates on the conditions of Qair=0 and 10SLM.

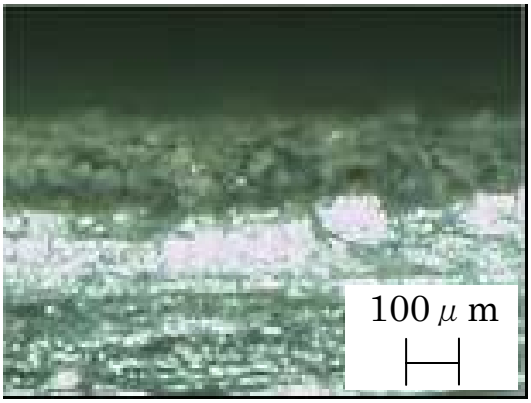

Q_{air}=0 SLM

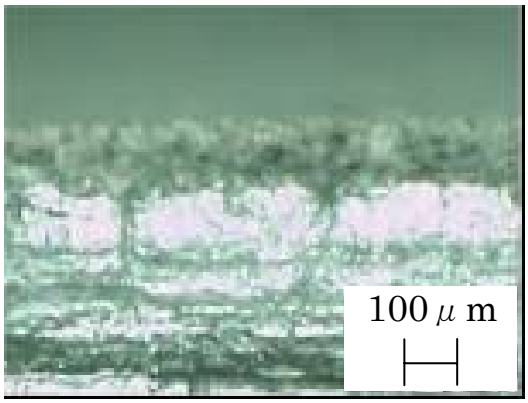

Q_{air}=10 SLM

Fig.10 Optical micrographs of the fracture cross-sections of the zinc oxide film deposited substrates on the conditions of Qair=0 and 10SLM.

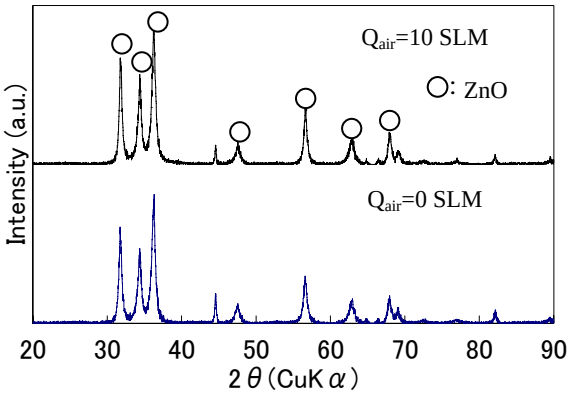

Fig.11 XRD patterns of the zinc oxide film deposited substrates on the conditions of Qair=0 and 10SLM.

3.4 Effect of air addition as working gas

Fig.12 shows appearances of the plasma jets using Ar and Ar/ air as working gases, respectively. In the case of air addition to the Ar plasma jet as carrier gas, the plasma jet could be maintained and the discharge voltage was kept at 25 V even at the condition of Q_{air}=40 SLM though the color of plasma jet was changed by air addition and the air was confirmed to be dissolved into the plasma. While, in the case of air addition to the Ar plasma jet as working gas, discharge voltage was dramatically raised from 25 V to 38.5 V at the condition of 2 SLM air addition but arc-suppression occurred at the condition of over 2 SLM air addition. From these results, it was proved that the behavior of the air in this case was far from that in the case of air addition as carrier gas.

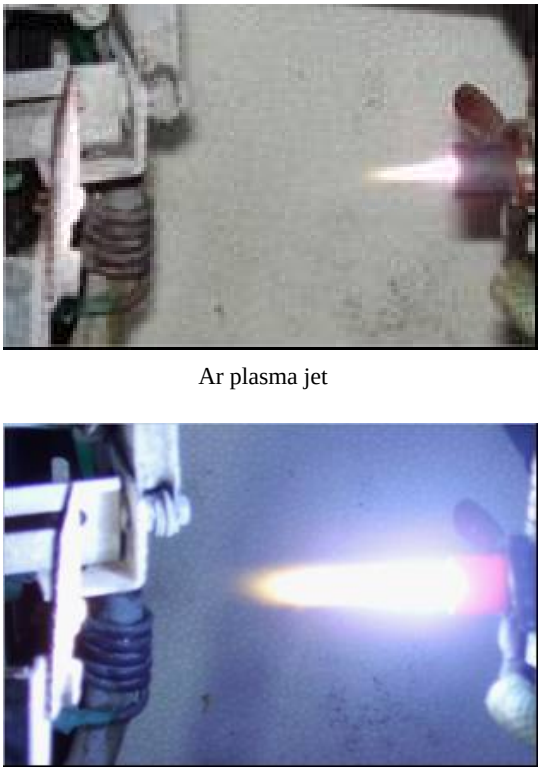

Ar plasma jet

Ar/ air plasma jet

Fig.12 Appearances of Ar and Ar/ air plasma jets.

4. Conclusions

In order to develop a high rate film deposition process and obtain photo-catalyst thick film with high strength, deposition of zinc oxide film by using atmospheric was carried out.

Consequently, 100 μm thick photo catalytic zinc oxide film could be deposited with only 5 min. deposition. In addition, in the case of air added Ar plasma jet as working gas, the discharge voltage was raised from 25 V to 38.5 V at the condition of 2 SLM air addition but arc-suppression occurred at the condition of over 2 SLM air addition. That is, the additional air as working gas showed a different behavior from that as carrier gas.

References

1) X.-L. Guo, J.-H. Choi, H. Tabata, T. Kawai, Jpn. J. Appl. Phys., 40 (2001) L177-L180.
2) H. Saitoh, T. Washio, S. Ohshio, Advances in Tech-nology of Materials and Materials Processing Journal, 6, 1 (2004) 47-52.
3) A W. J. E. Beek, M. M. Wienk, R. A. J. Janssen, Ad-vanced Materials, 16, 12 (2004) 1009–1013.
4) J-W. Bae, S-W. Lee, K-H. Song, J-I. Park, K-J. Park,Y-W. Ko, G-Y. Yeom, Jpn. J. Appl. Phys. 38, Pt. 1, 5A, (1999) 2917–2920.
5) H. Nanto, T. Minami, S. Shoji, S. Tanaka, J. Appl. Phys., 55 (1984) 1029 -1034.
6) T. Minami, H. Sato, H. Sonohara, S. Tanaka, T. Mi-yata, I. Fukuda, Thin Solid Film, 253 (1994) 14-19.
7) G. J. Exarhos, S. K. Sharma, Thin Solid Films, 270 (1995) 27-32.